5856 *Chem. Mater.* **2010,** *22,* 5856–5865
DOI:10.1021/cm101567v

CHEMISTRY OF MATERIALS
Article

Pulse Reactor Studies to Assess the Potential of $La_{0.75}Sr_{0.25}Cr_{0.5}Mn_{0.4}X_{0.1}O_{3-\delta}$ (X = Co, Fe, Mn, Ni, V) as Direct Hydrocarbon Solid Oxide Fuel Cell Anodes

Michael van den Bossche[†] and Steven McIntosh*[,†,‡]

[†]*Department of Chemical Engineering, University of Virginia, Charlottesville, Virginia 22904, United States, and* [‡]*Department of Chemical Engineering, Lehigh University, Bethlehem, Pennsylvania 18015, United States*

Received June 4, 2010. Revised Manuscript Received September 10, 2010

A pulse reactor technique was utilized to measure CH_4 oxidation rates under solid oxide fuel cell (SOFC) anode conditions. $La_{0.75}Sr_{0.25}Cr_{0.5}Mn_{0.4}X_{0.1}O_{3-\delta}$ powders (LSCMX, X = Co, Fe, Mn and Ni) were synthesized and were found to be phase-pure perovskites, space group $R\bar{3}C$. All compositions were determined by XRD to be stable up to 800 °C in dry 20% CH_4/N_2, at which point small amounts of a Ruddlesden-Poepper (RP) phase $A_2BO_{4-\delta}$ were detected. At higher temperatures, MnO and metallic Fe were observed, but no Ni and Co phases could be detected. Measurements of the CH_4 reaction rates on LSCMX samples provided indirect evidence for the instability of Ni and Co containing perovskites at temperatures higher than 650 and 750 °C, respectively. At 600 and 650 °C, CH_4 oxidation rates for LSCMCo and LSCMNi were similar to the rates on LSCM. At higher temperatures, CO_2 and CO production on LSCMCo and LSCMNi samples was enhanced, which was ascribed to the exsolution of Co and Ni from the perovskite lattice. CO_2 production rates on LSCM and LSCMFe continuously decreased with oxygen stoichiometry whereas LSCMCo and LSCMNi produced CO_2 in two separate regions of oxygen stoichiometry. The second region was attributed to the reduction of Co and Ni, respectively, present either as a metal oxide or in an RP phase. For all temperatures, LSCMFe had the lowest CH_4 reaction rate of the materials tested.

Introduction

Fuel cells are one of the most promising candidates for future power generation because of their high theoretical energy conversion efficiency and scalability. A variety of different fuel cells exist, differing in operating temperature, electrolyte and electrode composition, and the fuel they use. The distinguishing feature of solid oxide fuel cells (SOFCs) is the transportation of oxygen anions from the cell cathode to the anode through a dense ceramic electrolyte. This requires operating temperatures in the range of 700−1000 °C and provides the potential to utilize a wide range of fuels, including H_2, diesel, natural gas, and future biofuels. In the case of hydrocarbon fuels, oxidation at the anode can be complete or partial, depending on the catalyst material and the operating conditions. Hydrocarbon cracking can also occur, as well as secondary reactions between reactants and products of the oxidation reactions. Ideally, the SOFC anode material catalyzes complete oxidation, as this reaction represents full utilization of the energy potential of the fuel. The current research challenge is to create anode materials or composites[1,2] that will selectively catalyze this reaction, while providing the required high oxygen ion and electronic conductivity necessary to minimize ohmic losses. The material must also be stable at operating temperature and in atmospheres with partial oxygen pressure (pO_2) < 10^{-20} atm.

The perovskite-structured oxide $La_{0.75}Sr_{0.25}Cr_{0.5}Mn_{0.5}O_{3-\delta}$ (LSCM) has been reported as a promising anode material[3] and mitigates some of the main drawbacks of the traditional Ni/YSZ anode cermet, such as graphitic carbon formation,[4] sulfur poisoning,[5] and redox-cycling instability.[6] Oxygen diffusion and surface exchange coefficients are, however, low for LSCM,[7] and the power output of SOFC with LSCM anodes is typically lower than for fuel cells with Ni/YSZ cermets, although the latter have been optimized to a much greater extent than the LSCM-based anode. Previous work in our lab[8] has shown that the power output of a cell is higher in H_2 than in CH_4 and that the anode impedance increases from 0.66 to 0.80 to 1.71 Ω cm^2 when changing from H_2 to C_4H_{10} to CH_4

*To whom correspondence should be addressed. E-mail: mcintosh@lehigh.edu.

(1) Jacobson, A. J. *Chem. Mater.* **2009**, *22*(3), 660.
(2) Atkinson, A.; Barnett, S.; Gorte, R. J.; Irvine, J. T. S.; McEvoy, A. J.; Mogensen, M.; Singhal, S. C.; Vohs, J. *Nat. Mater.* **2004**, *3*(1), 17–27.
(3) Tao, S. W.; Irvine, J. T. S. *Nat. Mater.* **2003**, *2*(5), 320–323.
(4) Toebes, M. L.; Bitter, J. H.; van Dillen, A. J.; de Jong, K. P. *Catal. Today* **2002**, *76*(1), 33–42.
(5) Matsuzaki, Y.; Yasuda, I. *Solid State Ionics* **2000**, *132*(3−4), 261–269.
(6) Sarantaridis, D.; Atkinson, A. *Fuel Cells* **2007**, *7*(3), 246–258.
(7) Raj, E. S.; Kilner, J. A.; Irvine, J. T. S. *Solid State Ionics* **2006**, *177*(19−25), 1747–1752.
(8) Bruce, M. K.; van den Bossche, M.; McIntosh, S. *J. Electrochem. Soc.* **2008**, *155*(11), B1202–B1209.

 Published on Web 10/06/2010

fuel at 700 °C. Considering that the pO_2 and, hence, the electronic and oxygen ion conductivity of LSCM are similar for these fuels, the lower power output and higher impedance are expected to be because of the limited electrocatalytic activity of LSCM. Indeed, dense LSCM anodes did not catalyze the reaction of CH_4 at all at 700 °C[9] and LSCM powder was found to have a maximum reaction rate of only 1.7×10^{-3} mmol O^{2-} m^{-2} s^{-1} in 700 °C CH_4, compared to 28×10^{-3} mmol O^{2-} m^{-2} s^{-1} in H_2 at the same temperature.[10]

Several groups are pursuing routes to enhance the catalytic activity of LSCM. The addition of up to 1 wt % of a precious metal catalyst, such as Pt, Pd, or Rh to LSCM increased fuel cell performance[11] but may be prohibitively expensive for large power systems. Another strategy is to add up to 5 wt % of transition metals, such as Fe or Ni as a separate phase.[11,12] Although these materials are stable in the short term, their long-term mechanical stability is questionable because of the innate tendency of Ni and Fe to form graphitic carbon in dry hydrocarbons.[13] A third option is to replace all of the B-site Mn with other transition elements, but this either leads to lower reaction rates in the case of Ti or to instability of the perovskite in the case of Co.[14]

SOFCs with anodes made from the materials described in the previous paragraph did indeed have enhanced fuel cell performance (apart from Ti-substituted LSCM). However, it remains unclear what the effect is on the catalytic activity: do these materials enhance cracking, partial oxidation, or total oxidation of CH_4? What is the increase of CH_4 reaction rates relative to LSCM? To answer these questions, the formation rates of C, CO and CO_2 need to be determined.

Furthermore, it is essential to perform these measurements under conditions representative of the fuel cell anode environment. No gas-phase oxygen is present at the anode, and all oxygen is supplied as ions migrating through the anode material from the underlying electrolyte, hence the low equilibrium $pO_2 < 10^{-20}$ atm. Previous rate measurements that use a traditional mixture of air and CH_4 expose the catalyst to large amounts of oxygen, pO_2 O(10^{-1}) atm, or if gas phase fuel combustion occurs, high H_2O and CO_2 partial pressures.[13,15] The catalyst crystal structure, surface composition, and bulk oxygen stoichiometry are strongly dependent on pO_2, and these factors in turn influence catalytic activity. Therefore, the activity and selectivity of the anode catalysts can be very different when using a CH_4/air mixture instead of pure, dry, fuels. Measurements with no gas-phase oxygen supplied to the reactor then represent a true assessment of material performance in this extreme environment.

In the absence of gas-phase oxygen or oxygen ion supply, we expect that catalyst powders will be quickly depleted of near-surface oxygen. Oxygen present in the bulk of the catalyst will replenish the near-surface oxygen, but this supply is limited; furthermore, because of the modest oxygen ion conductivity of the catalysts, it is very likely that the diffusion of oxygen will limit the reaction rate of CH_4 even if only small amounts of CH_4 are continuously fed to the reactor.

To measure CH_4 oxidation rates that are indicative of the rates occurring on a working SOFC anode, we have developed a pulse-type experiment in which a reducing mixture of CH_4/Ar is fed to the catalyst in 6-s pulses, separated by 120-s intervals of pure Ar. During the pulses, CH_4 is oxidized by near-surface oxygen anions, which are replenished by bulk ion transport from the particle core during the 120-s interval. This setup allows for a controlled oxidation of CH_4, minimizing the influence of oxygen transport on the measured reaction rates. Furthermore, this method makes it possible to measure the catalytic activity and selectivity as a function of sample oxygen stoichiometry.

In this study we have synthesized the catalysts $La_{0.75}Sr_{0.25}Cr_{0.5}Mn_{0.4}X_{0.1}O_{3-\delta}$ (X = Co, Fe, Mn Ni and V) and assessed their potential as SOFC anode materials. The amount of B site substitution was limited to 10 mol % to enhance the catalytic activity of LSCM without significantly decreasing the materials' stability in reducing atmospheres. The substituents have previously been reported to enhance CH_4 oxidation and cracking[11,12,14] or, in the case of V, sulfur tolerance[16] and reforming.[17] The stability, selectivity and methane oxidation rates were determined under anode operating conditions and compared to LSCM.

Experimental Section

Synthesis. $La_{0.75}Sr_{0.25}Cr_{0.5}Mn_{0.4}X_{0.1}O_{3-\delta}$ (X = Co, Fe, Mn, Ni, and V, denoted LSCMX in the following) powders were synthesized utilizing a modified Pechini method[18] (Table 1). Aqueous solutions of La, Sr, Mn, Ni (> 99% pure, Alfa Aesar), Co, Fe (> 99% pure, Acros Organics), and Cr nitrate salts (> 99% pure, Strem) were prepared, and the metal concentrations determined by titration. For vanadium, an aqueous solution of metavanadate ammonium salt (99.995% pure, Alfa Aesar) was used as a precursor. Solutions were mixed in the appropriate molar ratios with the chelating agent EDTA, after which excess water was evaporated to form a homogeneous gel. The gel was pyrolyzed at 300 °C, followed by firing of the resulting powder for 4 h at 1000 °C, or 1100 °C in the case of LSCMFe, to form the perovskite phase. The powder was sieved to obtain the 106−212 μm size fraction, which was used for all

(9) van den Bossche, M.; Matthews, R.; Lichtenberger, A.; McIntosh, S. *J. Electrochem. Soc.* **2010**, *157*(3), B392–B399.
(10) van den Bossche, M.; McIntosh, S. *J. Catal.* **2008**, *255*(2), 313–323.
(11) Kim, G.; Lee, S.; Shin, J. Y.; Corre, G.; Irvine, J. T. S.; Vohs, J. M.; Gorte, R. J. *Electrochem. Solid State Lett.* **2009**, *12*(3), B48–B52.
(12) Liu, J.; Madsen, B. D.; Ji, Z. Q.; Barnett, S. A. *Electrochem. Solid State Lett.* **2002**, *5*(6), A122–A124.
(13) Sfeir, J.; Buffat, P. A.; Mockli, P.; Xanthopoulos, N.; Vasquez, R.; Mathieu, H. J.; Van herle, J.; Thampi, K. R. *J. Catal.* **2001**, *202*(2), 229–244.
(14) Danilovic, N.; Vincent, A.; Luo, J.-L.; Chuang, K. T.; Hui, R.; Sanger, A. R. *Chem. Mater.* **2009**, *22*(3), 957.
(15) Tao, S. W.; Irvine, J. T. S.; Plint, S. M. *J. Phys. Chem. B* **2006**, *110*(43), 21771–21776.
(16) Peng, C.; Luo, J. L.; Sanger, A. R.; Chuang, K. T., *Chem. Mater.* *22*, (3), 1032-1037.
(17) Vernoux, P.; Guillodo, M.; Fouletier, J.; Hammou, A. *Solid State Ionics* **2000**, *135*(1−4), 425–431.
(18) van Doorn, R. H. E.; Kruidhof, H.; Nijmeier, A.; Winnubst, A. J. A.; Burggraaf, A. J. *J. Mater. Chem* **1998**, No. 8, 2109–2112.

Table 1. XRD and BET Results for as Prepared LSCMX (X = Mn, Co, Fe, Ni)

sample	composition	T_{calcd} [°C]	space group	lattice parameter [Å] $a = b$	lattice parameter [Å] c	V [Å^3]	BET [m^2/g]
LSCM	$La_{0.75}Sr_{0.25}Cr_{0.5}Mn_{0.5}O_{3-\delta}$	1000	$R\bar{3}C$	5.523(1)	13.40(0)	354.0	4.44
LSCMCo	$La_{0.75}Sr_{0.25}Cr_{0.5}Mn_{0.4}Co_{0.1}O_{3-\delta}$	1000	$R\bar{3}C$	5.515(6)	13.38(7)	352.7	4.74
LSCMFe	$La_{0.75}Sr_{0.25}Cr_{0.5}Mn_{0.4}Fe_{0.1}O_{3-\delta}$	1100	$R\bar{3}C$	5.524(2)	13.40(5)	354.3	2.86
LSCMNi	$La_{0.75}Sr_{0.25}Cr_{0.5}Mn_{0.4}Ni_{0.1}O_{3-\delta}$	1000	$R\bar{3}C$	5.518(6)	13.39(1)	353.2	5.93

characterization experiments. LSCM with 9 mol % of NiO as a separate phase (referred to as LSCM + Ni) was prepared by adding 0.6 mL of a 0.18 M $Ni(NO_3)_2$ solution to 0.25 g of LSCM powder, followed by evaporation of the water and firing at 800 °C to form NiO.

Characterization. Powder X-ray diffraction patterns were collected using CuKα radiation with fixed slit width (Scintag X-ray Diffraction XDS 2000). Diffraction patterns were recorded in the 2θ range of 20−65° using a counting time of 1 min/deg and a 0.02° step size. Rietveld structural refinements were carried out using the GSAS package.[19] BET surface area measurements (Micromeritics ASAP 2020) were carried out using N_2 as the adsorbent, after degassing samples at 400 °C for 6 h. Thermogravimetric analysis (TA Instruments, SDT Q600) was used to determine the change in oxygen stoichiometry of the samples. Powders were treated in air for 30 min at 700 °C and cooled at a rate of 5 °C/min to remove surface carbonates before measuring. The sample mass, initially between 6 and 14 mg, was recorded as a function of temperature, equilibrating for 8 h at each 50 °C increment from 600 to 850 °C, and for 48 h at 1000 °C, in both 100 mL/min N_2 and 100 mL/min 5% H_2/N_2 (UHP gases, < 2 ppm O_2, GTS-Welco). The mass stabilized to within the accuracy range (0.1 μg) of the instrument during the dwells. The surface of LSCM and LSCMNi particles was studied before and after treatment in 700 °C dry 20% CH_4/N_2 utilizing Transmission Electron Microscopy (TEM) (JEOL 2000FX). Samples were prepared by dispersing powders in ethanol and depositing them onto a Cu grid with a lacy carbon support film. X-ray Photoelectron Spectroscopy (XPS) (PHI Quantera SXM) measurements were performed in the 0−1.1 keV range, using monochromatic Al X-rays. LSCMCo and LSCMNi samples were measured as-prepared and annealed in 20% dry H_2/N_2. Annealing temperature was 800 °C for LSCMCo and 700 and 800 °C for LSCMNi.

Pulse Reactor Experiments. CH_4 reaction rates were determined using the pulse setup described earlier.[10] LSCMX powder (0.12 g) was placed in a 1/4 in. (6.4 mm) i.d. quartz tube and held in place with quartz glass wool. Measurements were performed at each 50°C increment from 600 to 850°C. The quartz reactor was heated to the measurement temperature or to 700°C, whichever was higher, while feeding 20 mL/min 10.1 vol% O_2/N_2 (GTS-Welco) over the sample to remove surface carbonates and to oxidize the powder. The reactor was subsequently brought to the reaction temperature and flushed for 2 h with 50 mL/min Ar (UHP, < 1 ppm O_2, GTS-Welco) to ensure that the sample oxygen stoichiometry was fully equilibrated with the O_2 present in the Ar stream before measuring. After 2 h, only baseline O_2 was present in the reactor effluent. The sample was then exposed to up to 300 6-s pulses of 20 vol% CH_4/Ar (UHP gases, < 5 ppm O_2, GTS-Welco) flowing at 50 mL/min. The pulses were separated by 120-second intervals of 50 mL/min Ar. Well-defined and repeatable pulses were achieved by using a 4-way computer-controlled solenoid valve (Swagelok model 131 SR). The reactor effluent was continuously analyzed with a sampling rate of 2.2/s using an in-line mass spectrometer (Pfeiffer Vacuum, Omnistar GSD300). During the pulses, CH_4 reacted with the oxygen present in the lattice of the catalyst powder to form the total oxidation products (CO_2 and H_2O) or partial oxidation products (CO and H_2). Quantification of the reactor products was accomplished by calibration of the mass spectrometer signals m/e = 28 (CO, N_2) and m/e = 44 (CO_2) in the range of 0.013 to 80 vol % CO or CO_2 in 20 vol% CH_4/Ar. The amounts of CO_2 (and implied H_2O) and CO produced in a pulse were used to calculate the total oxygen consumed and hence the change in oxygen stoichiometry of the sample per pulse. In this way, the rate of CO_x production was measured as a function of sample oxygen stoichiometry with each pulse reducing the oxygen stoichiometry by a small amount. The CH_4 pulse duration was selected to minimize the change in oxygen stoichiometry per pulse.

It was not possible to detect cracking during the pulsing experiments, since the generated carbon was deposited onto the sample and remained in the reactor. Instead, the amount of cracking was estimated during reoxidation of the sample. After the pulse experiment at one temperature, the reactor was cooled down, and the sample was reoxidized to start the pulsing experiment at the next 50 °C increment. Carbon deposited during the previous pulsing experiment was released as CO_2 during reoxidation and quantified using calibration data for CO_2 in 10.1 vol% O_2/N_2.

Results

As-prepared LSCM and LSCM with 10 mol % Co, Fe and Ni substituted on the B-site, were indexed as phase-pure rhombohedral perovskites, space group $R\bar{3}C$ (Figure 1). LSCMFe had to be calcined at 1100 °C to obtain a pure perovskite. LSCMV contained a secondary phase that could not be attributed to a perovskite or a vanadia phase. This phase remained present after treatment of the fired LSCMV powder in 800 °C humidified 20% H_2/N_2 but was removed by reduction in 1000 °C dry 20% H_2/N_2. The latter treatment also led to the formation of a Ruddlesden-Poepper (RP) phase. No subsequent attempts were made to synthesize phase-pure LSCMV. XRD patterns were fitted using Rietveld structural refinements (table 1), with X^2 values, a measure of the error between the calculated and the recorded pattern, ranging from 1.10 to 1.21, indicating an appropriate fit. The unit cell volume changed only slightly with composition, increasing in the order Co < Ni < Mn < Fe. BET surface areas (table 1) ranged from 2.86 m^2/g for LSCMFe to 5.93 m^2/g for LSCMNi. The low surface area for LSCMFe was attributed to the higher firing temperature, 1100 °C instead of 1000 °C.

The stability of the substituted lanthanum chromates was investigated by treating LSCMX powders (I) for 16 h

(19) Larsen, A. C.; von Dreele, R. B., *General Structure Analysis System (GSAS)*; Report LAUR B6-748; Los Alamos National Laboratory: Los Alamos, NM, 1985.

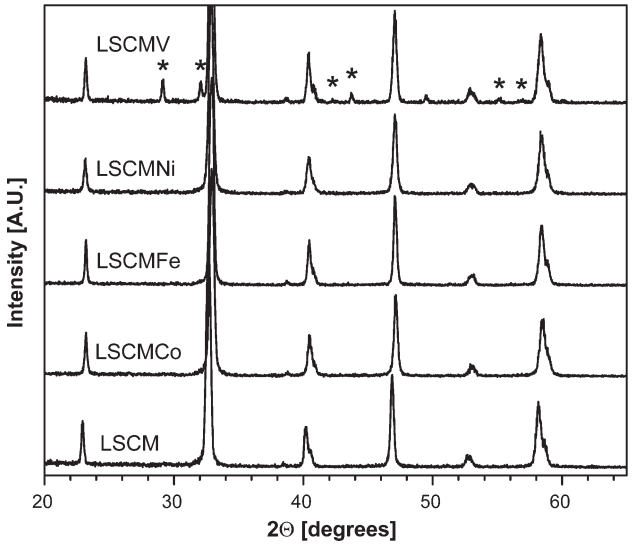

Figure 1. X-ray diffraction patterns for as prepared LSCMX. Asterisk (*) indicates an unknown secondary phase.

in 650 °C dry CH_4/N_2, (II) for 12 h in 850 °C humidified 20% H_2/N_2 (Figure 2a), and (III) for 16 h in 1000 °C dry H_2/N_2, and collecting XRD patterns. Additional measurements were performed for LSCM reduced in dry CH_4/N_2 at 750, 800, and 850 °C (Figure 2b). Although treatment at 650 °C (shown for LSCM in Figure 2b) resulted in a phase change from rhombohedral $R\bar{3}C$ to orthorhombic *Pbnm*, all compositions remained phase-pure perovskites. In samples treated in 850 °C humidified H_2, a mixture was detected, consisting of mainly orthorhombic perovskite with traces of an $A_2BO_{4-\delta}$ RP phase, space group *I*4/*mmm* (Figure 2a). No metal or metal-oxide phases were observed. The same phases were also found in dry CH_4, starting at 800 °C (Figure 2b). All compositions reduced at 1000 °C (shown for LSCM in Figure 2b) contained perovskite, RP and MnO phases, and an additional Fe phase was observed for LSCMFe. No additional peaks were recorded for LSCMNi and LSCMCo.

Thermogravimetric analysis (TGA) was performed in 5% H_2/N_2 and pure N_2 atmospheres from room temperature to 1000 °C. No significant weight loss was detected in N_2, as expected from previously reported results.[20] The decrease in mass in H_2/N_2 was similar for all samples, 4.4% of the initial mass, equivalent to the release of 0.62−0.64 mols of oxygen per mol of perovskite (Table 2), in excellent agreement with the 4.5% previously reported for LSCM in 5% CH_4.[14] As noted above, reduction of the materials in 1000 °C dry H_2/N_2 for 16 h yields a mixture of perovskite, Ruddlesden−Poepper and manganese oxide phases, with unknown oxygen content. This prevents assigning an absolute value to the oxygen stoichiometry. As such, only the change in oxygen stoichiometry is reported in this work.

Next, CH_4 reaction rates on the LSCMX powders were measured at temperatures from 600 to 850 °C, using the pulsing technique described in the Experimental Section. Qualitatively, all samples produced CO_2 in conjunction with H_2O (total oxidation products) or CO together with H_2 (partial oxidation products). Figure 3a−f shows CO_2 production rates as a function of oxygen content for different LSCMX materials at temperatures ranging from 600 to 850 °C. The oxygen content of the samples, shown

(20) Oishi, M.; Yashiro, K.; Sato, K.; Mizusaki, J.; Kawada, T. *J. Solid State Chem.* **2008**, *181*(11), 3177–3184.

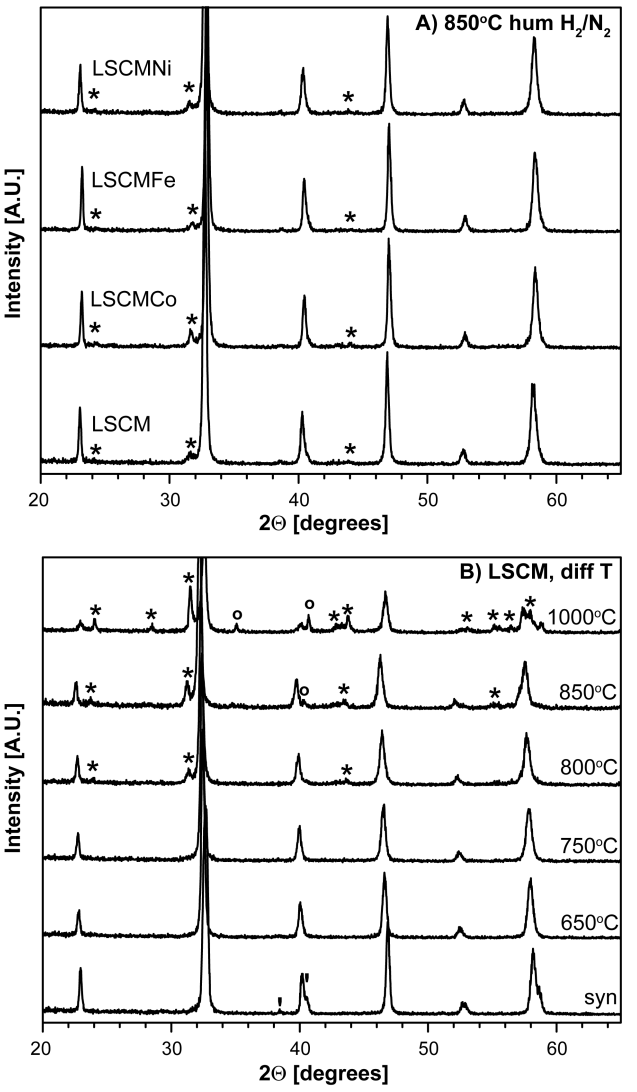

Figure 2. XRD patterns for (A) LSCMX treated for 12 h in 850 °C humidified H_2/N_2 and (B) LSCM, as prepared and reduced in 650, 750, 800, and 850 °C dry CH_4/N_2 and 1000 °C dry H_2/N_2. Peaks are labeled (′) rhombohedral $R\bar{3}C$, (*) RP, and (°) MnO.

Table 2. Cumulative Decrease in Oxygen Stoichiometry for LSCMX as a Function of Temperature in Dry 5% H_2/N_2 as Measured by TGA

T [°C]	ΔO LSCM [mol O/mol LSCM]	ΔO LSCMCo [mol O/mol LSCMCo]	ΔO LSCMFe [mol O/mol LSCMFe]	ΔO LSCMNi [mol O/mol LSCMNi]
25	0.00	0.00	0.00	0.00
600	0.16	0.20	0.18	0.18
650	0.19	0.21	0.18	0.20
700	0.21	0.22	0.18	0.21
750	0.22	0.23	0.18	0.23
800	0.24	0.25	0.18	0.25
850	0.29	0.31	0.24	0.32
1000	0.64	0.63	0.64	0.62

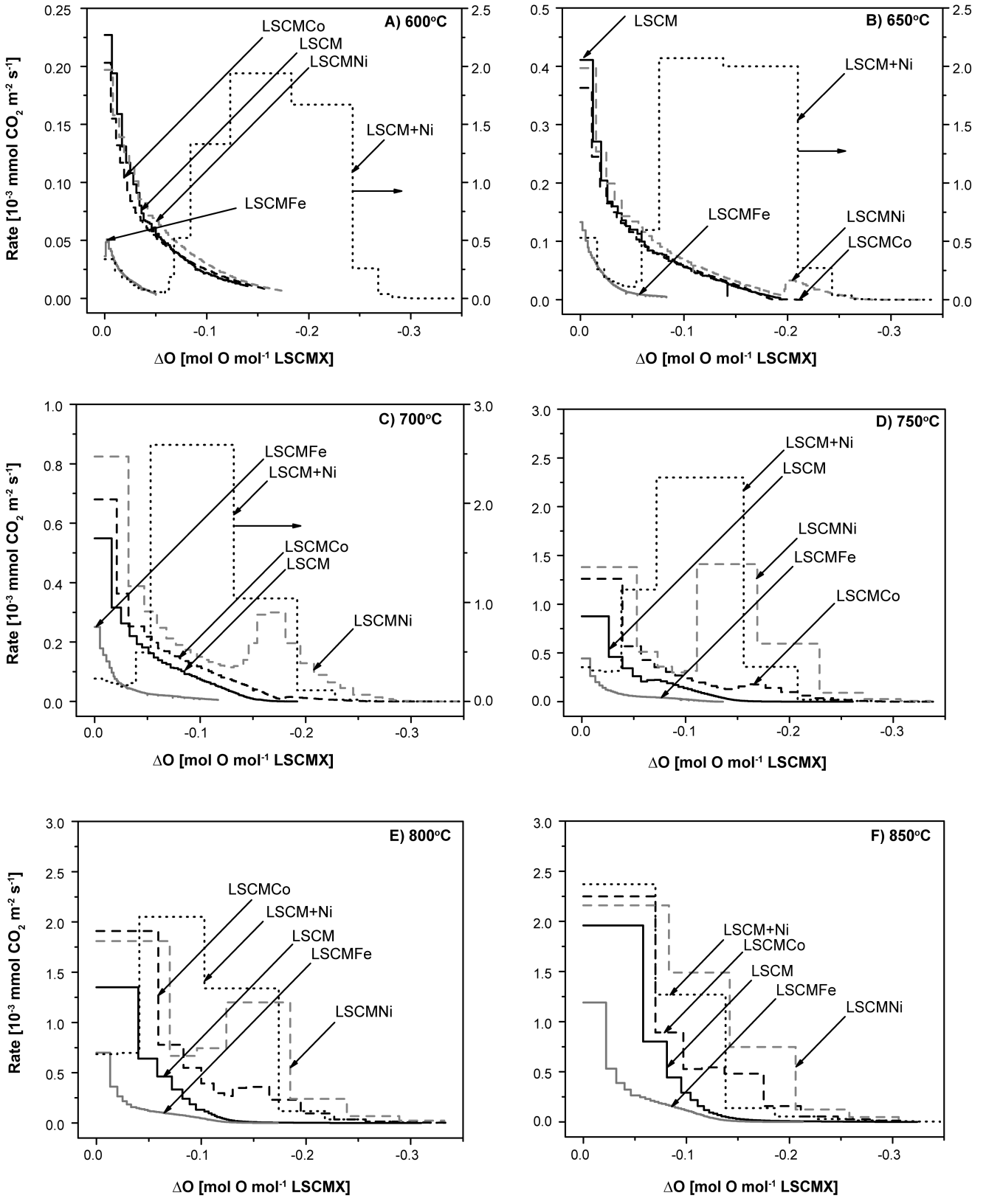

Figure 3. CO_2 production rates at temperatures ranging from 600 to 850 °C, for LSCM (black solid line), LSCMCo (black dashed line), LSCMFe (gray solid line), LSCMNi (gray dashed line), and LSCM+Ni (black dotted line). Note that for figures A to C, LSCM+Ni is shown on the right axis.

on the *x*-axis in moles of oxygen per mole of perovskite, was set to zero for the fully oxidized samples, and decreased over the course of the experiment. Rates for the LSCM+Ni cermet, consisting of 91 mol % LSCM and 9 mol % NiO, are expressed per mole of perovskite. The stepwise nature of the figures is the result of the stepwise nature of the experiment, with each step representing a single pulse of CH_4. Note that in Figure 3a−c the production rates for LSCM+Ni were much larger than for the other catalysts, and are therefore shown on the

right axis. Overall, CO_2 production rates increased with increasing temperature and depended on composition: LSCMNi > LSCMCo > LSCM > LSCMFe.

For all temperatures, CO_2 production rates on LSCM and LSCMFe continuously decreased over an oxygen stoichiometry range from 0 to −0.2 mol O/mol LSCMX. LSCMNi showed a similar decreasing trend at 600 °C, but at 650 °C, a second CO_2 production peak was measured, starting at an oxygen content of −0.20 mol O/mol LSCMNi. This peak was smaller than the initial CO_2 peak, but its magnitude increased with temperature. The position where the peak occurred shifted to higher oxygen contents for higher temperatures, until the peak merged with the initial peak to form one CO_2 production peak at 850 °C. Similar trends were observed for LSCMCo and LSCM+Ni, with two separate CO_2 production peaks first occurring at 750 and 600 °C, respectively.

CO production rates are shown in Figure 4a−c. For all temperatures, the production of CO increased in the order LSCMFe < LSCM ≪ LSCMCo < LSCMNi < LSCM+Ni. CO production rates increased with temperature, as expected. At 600 °C, none of the single-phase materials produced any measurable amount of CO. LSCM+Ni, however, started producing CO at −0.08 mol O/mol LSCM+Ni, at a maximum rate of 2.5×10^{-3} mmol m^{-2} s^{-1}. This rate increased with increasing temperature before stabilizing at $\sim 6 \times 10^{-3}$ mmol m^{-2} s^{-1} at 750 °C. LSCMNi and LSCMCo started producing CO at 650 °C, at a rate of 0.20 and 0.08×10^{-3} mmol m^{-2} s^{-1}, respectively. LSCM only produced significant amounts of CO at 800 °C and above, whereas CO production on LSCMFe is negligible at all measured temperatures.

As mentioned in the introduction, LSCM is a modest oxygen ion conductor. The primary reason to use a pulse approach is to ensure that we are measuring a surface that is equilibrated with the oxygen stoichiometry of the bulk. Re-equilibration occurs during the Ar dwell between pulses. If we utilize a continuous flow of CH_4, we would create a particle with an oxygen depleted shell and oxygen-rich core, thus risking measuring only the rate of oxygen transport from the core to the particle surface. To confirm that our approach was appropriate, the oxygen reaction rates for the reaction of CH_4 on LSCM at 800 °C, calculated from the CO_2 and CO production rates, were compared for time intervals between pulses of 120 and 3600 s (Figure 5). Within experimental error, the oxygen reaction rate for the experiment with 3600s pulse intervals was equal to the rate obtained using 120s intervals, indicating that the pulsing experiments were not diffusion limited and that our measurements represent surfaces equilibrated with the reported bulk oxygen stoichiometry.

Arrhenius curves further illustrated the difference in CO_2 production rates of the fully oxidized samples (Figure 6). Single straight lines could be fitted through the production rate values on LSCM and LSCMFe; for LSCMCo and LSCMNi the fit was much better when using two straight lines. At low temperatures, the trendline slopes for LSCMCo and LSCMNi are similar to the slope of LSCMFe, but at higher temperatures, the slopes

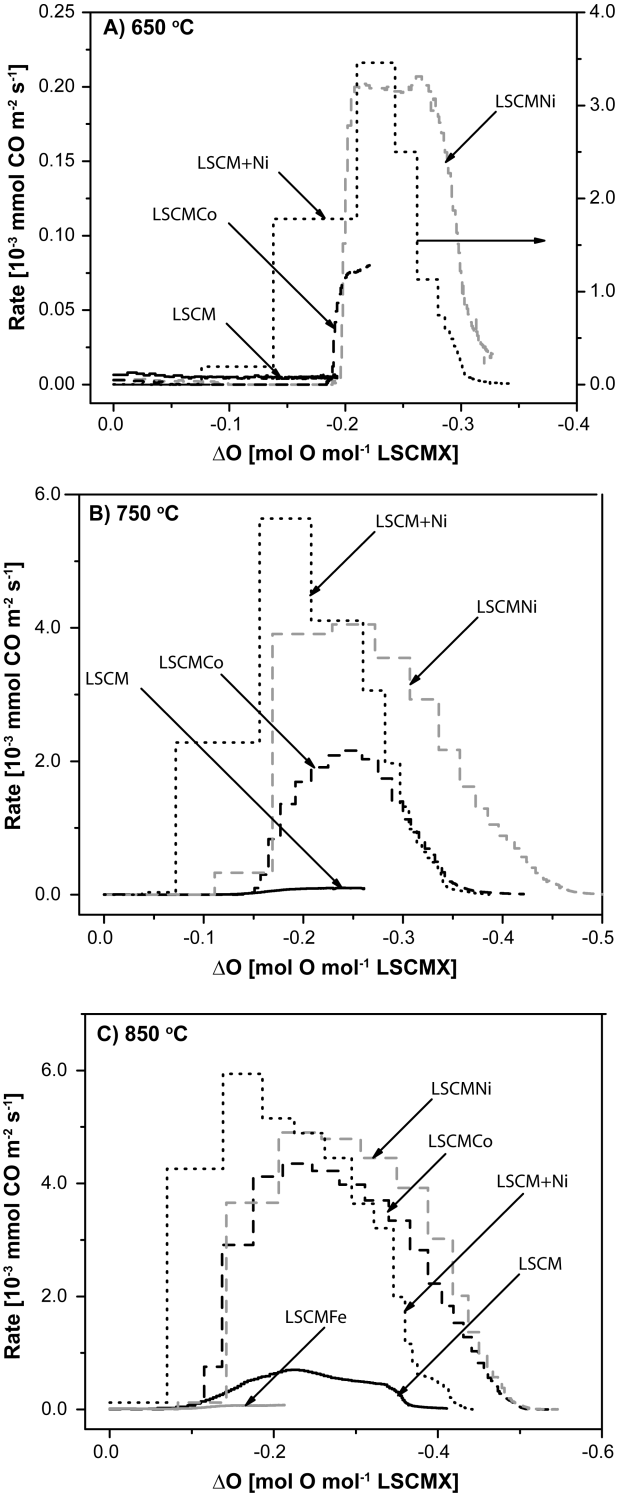

Figure 4. CO production rates at (A) 650, (B) 750, and (C) 850 °C, for LSCM (solid black), LSCMCo (dashed black), LSCMFe (solid gray), LSCMNi (dashed gray), and LSCM+Ni (dotted). Note that in panel A the rate for LSCM+Ni is shown on the right *y*-axis.

for the Co- and Ni-containing perovskites become shallower. This transition occurred after 700 and 750 °C for LSCMNi and LSCMCo, respectively.

Reoxidized LSCMNi samples that were previously exposed to high temperature reducing atmospheres, demonstrated CO_2 release and CO production characteristics similar to the LSCM+Ni sample at lower temperatures

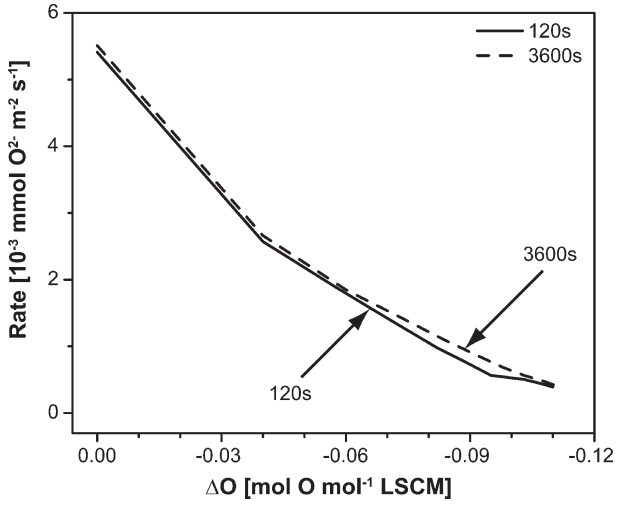

Figure 5. O^{2-} reaction rates on LSCM at 800 °C in CH_4 for interval times between pulses of 120 s (solid line) and 3600 s (dashed line).

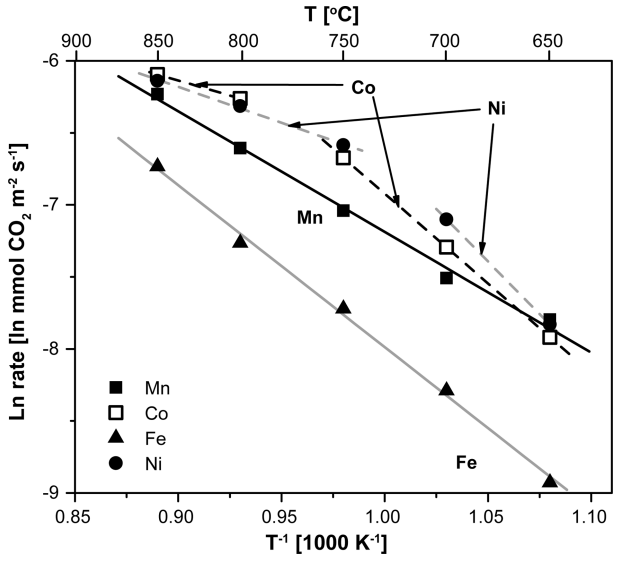

Figure 6. Arrhenius plot for initial CO_2 production rates on LSCM (■, black solid line), LSCMCo (□, black dashed line), LSCMFe (▲, gray solid line), and LSCMNi (●, gray dashed line).

than the as-prepared LSCMNi samples, Figure 7. At 600 °C, reoxidized LSCMNi that was previously reduced at 850 °C, produced CO_2 in two distinct peaks (Figure 7a) and produced significant amounts of CO (Figure 7b), similar to LSCM+Ni. CO_2 production on as-prepared LSCMNi continuously decreased with oxygen content and no CO was produced. Similar results were observed at measurement temperatures of 550 °C for LSCMNi and at 700 °C for LSCMCo (not shown).

From Figure 7, it was observed that the initial CO_2 production rate was higher on LSCMNi previously treated in reducing atmosphere than on untreated LSCMNi. This was further investigated by comparing the CO_2 production rates at 850 °C of as-prepared LSCMNi and LSCMNi previously tested at 650 and 800 °C (Figure 8). CO_2 production was lowest for the untreated sample, slightly increased for the sample previously tested at 650 °C, and was highest for LSCMNi previously tested at

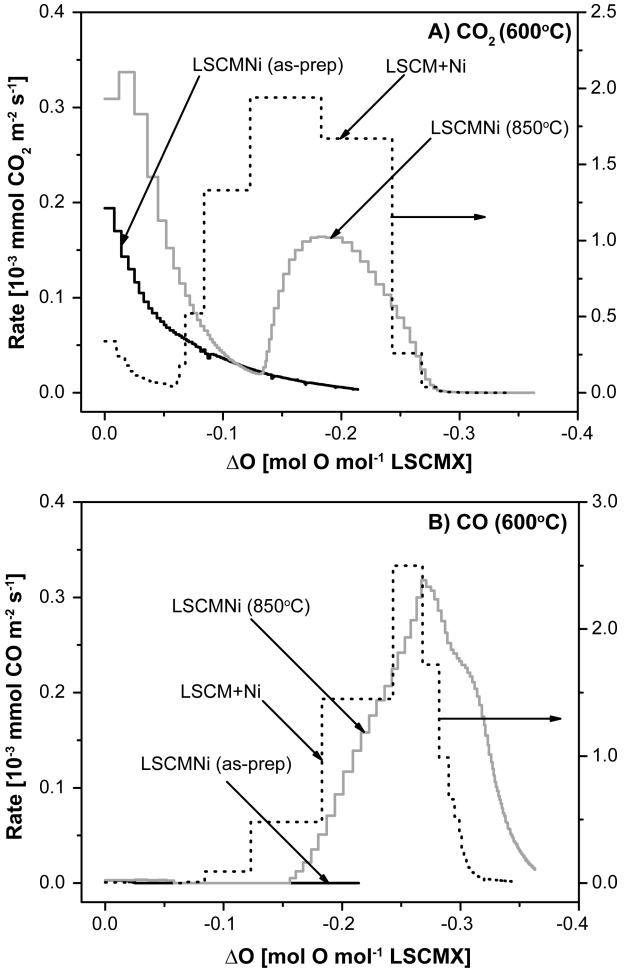

Figure 7. (A) CO_2 and (B) CO production rates at 600 °C for fresh LSCMNi (black line), LSCMNi previously tested at 850 °C (gray line), and LSCM with Ni added as a secondary phase (dotted line). Note that LSCM+Ni is shown on the right axis.

800 °C, with the latter showing an increase in CO_2 production rate of 20% compared to as-prepared LSCMNi.

Changes in the structure and in the elemental composition of the surface of the LSCMNi and LSCMCo powders were investigated using TEM and XPS. TEM images were taken at 80 000× magnification for LSCM (Figure 9a) and LSCMNi (b) after annealing in 700 °C dry CH_4/N_2 for 24 h and compared with as-prepared LSCMNi (c). LSCMX particles varied in size from 40 to 100 nm and were covered with smaller particles, 4 to 13 nm in size. Although most numerous on the annealed samples, all powders contained these small particles.

There was significant overlap between La, Mn and Ni energies in the XPS spectra of LSCMNi samples. This overlap, combined with the observation from high resolution XPS that Ni is only present in amounts close or equal to the limit of detection, Figure 10, prevented the identification of a trend in Ni surface concentration with reduction temperature. A similar overlap between Co and La peaks was observed for the LSCMCo samples, again with Co only present in small amounts. Furthermore, it was observed that Sr and Cr surface concentrations increased after reduction at 700 °C, and were enhanced further after reduction at 800 °C.

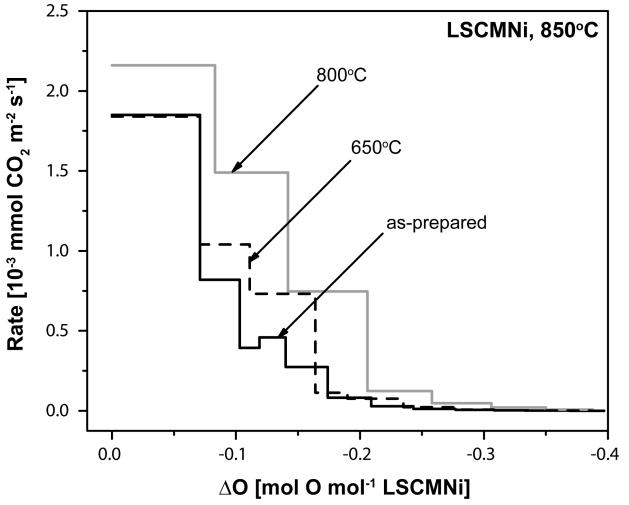

Figure 8. CO_2 production rates at 850 °C for fresh LSCMNi (black solid line), LSCMNi previously tested at 650 °C (black dashed line), and LSCMNi previously tested at 800 °C (gray solid line).

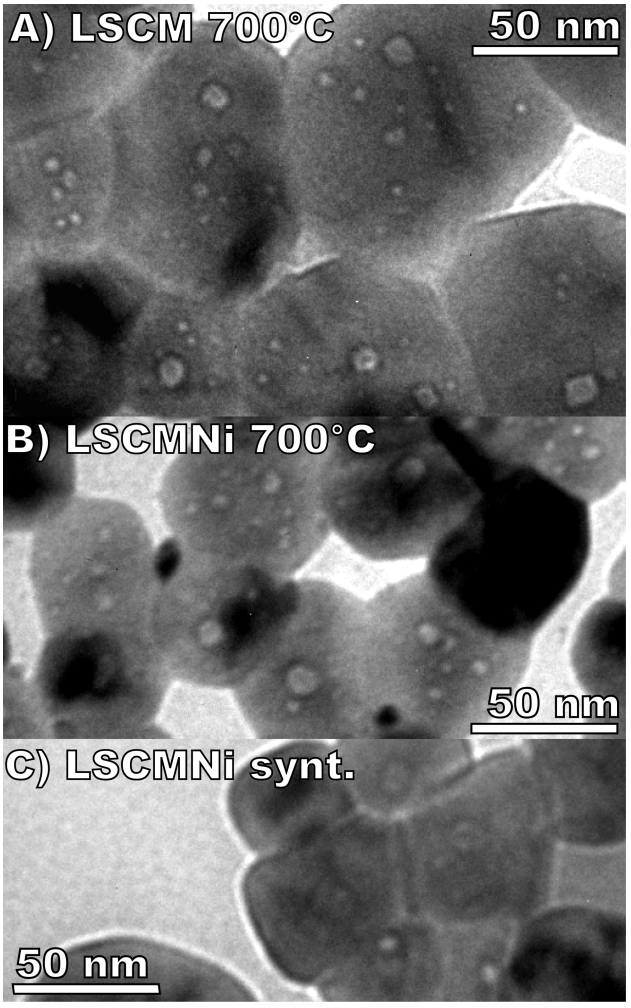

Figure 9. TEM images taken at 80 000× magnification of (a) LSCM and (b) LSCMNi, both after annealing in 700 °C dry CH_4/N_2 for 24 h, and (c) LSCMNi as prepared.

Lastly, the amount of cracking during the rate measurements was studied. This rate is an average over the total time that CH_4 was supplied to the sample during the pulsing experiments (Figure 11). All cracking is expected

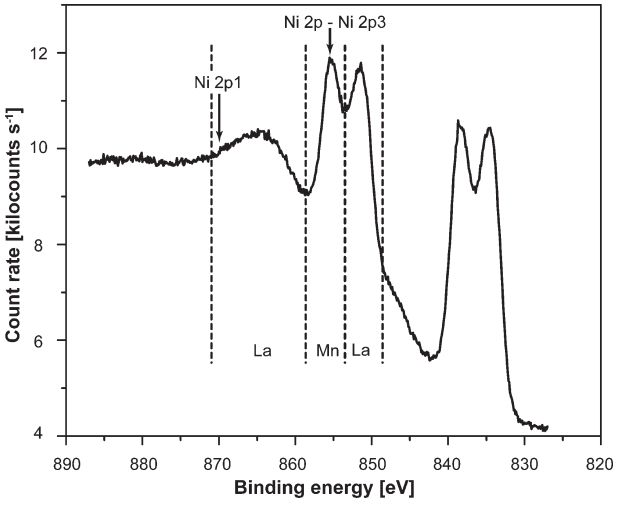

Figure 10. XPS spectrum for LSCMNi, annealed at 800 °C in dry 20% H_2/N_2. Arrows indicate the (small) peaks associated with Ni, while the dotted lines show the boundaries of the large, overlapping La and Mn peaks.

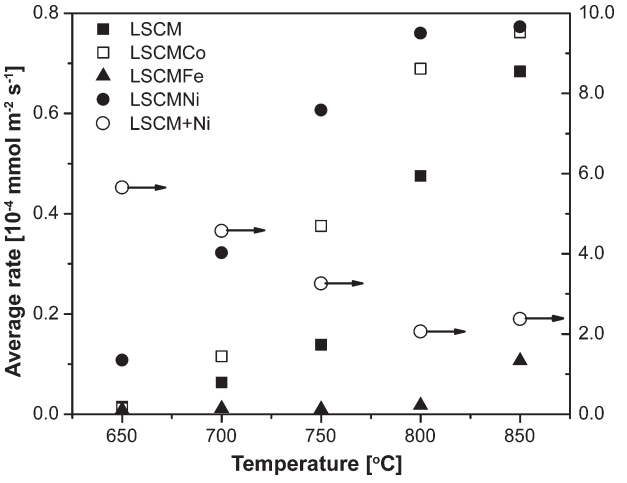

Figure 11. Carbon production rates averaged per pulse for LSCM (■), LSCMCo (□), LSCMFe (▲), LSCMNi (●), and LSCM+Ni (○). Note that the latter is shown on the right axis.

to occur on the sample surface, since no gas-phase cracking was observed when feeding CH_4 to a blank reactor up to 1000 °C. Compared to LSCM, cracking is inhibited on LSCMFe and enhanced on LSCMCo and LSCMNi. This is especially true at lower temperatures (650 and 700 °C), where cracking rates on LSCMCo and LSCMNi are up to seven times larger than for LSCM. For higher temperatures, cracking rates on LSCM increase, and at 850 °C, rates are similar for all single-phase materials. LSCM+Ni produced significantly more carbon than any of the other compounds, especially at lower temperatures.

Discussion

LSCMX compounds (X = Co, Fe, Mn, and Ni) were synthesized as phase-pure perovskites and fitted to the rhombohedral space group $R\bar{3}C$, in agreement with neutron diffraction data for LSCM.[21] The change in lattice

(21) Tao, S.; Irvine, J. T. S. *Chem. Mater.* **2006**, *18*(23), 5453.

volumes with substitution of Mn was small because the ionic radii of the substituting elements are very similar,[22] and there was only 10 mol % of substitution. The phase change from rhombohedral to orthorhombic after reduction in 650 °C dry CH_4/N_2 was previously observed by Bastidas et al for LSCM under similar conditions.[23] Also, the formation of an RP and an MnO phase after reduction of LSCMX at 800 and 850 °C, respectively, was previously reported for LSCM reduced in 900 °C H_2.[20] All LSCMX samples reduced at 1000 °C in humidified H_2/N_2 contained perovskite, RP, and MnO phases, and an additional peak, indexed to metallic Fe, was found for LSCMFe. No additional peaks were observed for LSCMCo and LSCMNi. Since perovskites containing Co and Ni were reported to be less stable than Fe and Mn,[24] metallic Co and Ni phases were expected to be present in the respective samples, probably at too low a concentration to be detected by XRD. TEM and XPS measurements did not yield proof for the presence of Co- and Ni-enriched phases on the powder surface after high-temperature reduction, but rate and selectivity measurements provided indirect evidence for the exsolution of Co and Ni from their respective perovskites and their enrichment at the reaction area.

CO_2 and CO production rates on LSCMX were measured as a function of oxygen stoichiometry at temperatures ranging from 600 to 850 °C. Rates for LSCM were in excellent agreement with the rates measured in our previous article: 1.4×10^{-3} compared to 1.7×10^{-3} mmol $m^{-2}\,s^{-1}$ for the initial CO_2 production rate at 800 °C, for example.[10] Also, the decrease in CO_2 production rates with decreasing oxygen stoichiometry, followed by the production of CO observed for LSCM was similar to the trends previously measured for $La_{0.75}Sr_{0.25}Cr_xMn_{1-x}O_{3-\delta}$[10] and is in agreement with a modified Mars-van Krevelen mechanism with Mn as the redox-active center.

None of the pulse measurements were limited by the supply of fuel. Even when measuring LSCM+Ni or LSCMNi at 850 °C, maximum CH_4 conversion was estimated to be <50%. Re-equilibration of the oxygen stoichiometry of the sample surface with that of the bulk material between pulses was also not a limiting factor, as demonstrated by the similarity in CH_4 oxidation rates on LSCM at 800 °C using 2 and 60 min interval times. Previous measurements comparing the reaction rates of H_2 and CH_4 fuel on LSCM[10] showed a maximum oxygen reaction rate of 28×10^{-3} mmol $O^{2-}\,m^{-2}\,s^{-1}$ for 700 °C H_2, much higher than the maximum rate of 9.2×10^{-3} mmol $O^{2-}\,m^{-2}\,s^{-1}$ found in this article for the oxidation of CH_4 fuel on LSCM+Ni at 850 °C. Since bulk ion diffusion may be considered independent of fuel (because of the similar gas-phase pO_2), this further indicates that the CH_4 reaction rates reported here are surface reaction limited, not ion or gas-phase diffusion limited. Finally, measurements with 2.7 wt % Pt added to the LSCM surface showed an increase in CH_4 oxidation rates by factors of 29, 6.7, and 1.7 for temperatures of 600, 700, and 800 °C, respectively.[10] The combination of these measurements supports that we are measuring surface reaction limited rates for CH_4 oxidation on these materials, up to at least 800 °C.

During the pulsing experiments, the oxygen stoichiometry decreased continuously and reached a final value at the end of the experiment which is in reasonable agreement with values measured for the oxygen loss in 5% H_2/N_2 using TGA. For LSCM at temperatures between 600 and 700 °C, TGA values measured with H_2 are up to 0.02 mol O/mol LSCM higher than the oxygen losses measured for the pulsing experiments. At higher temperatures, the oxygen losses calculated from the pulsing experiments became larger than the values measured with TGA, but they never exceeded the values for the oxygen losses measured at 1000 °C in 5% H_2/N_2. LSCMCo and LSCMNi showed the same behavior as LSCM; for LSCMFe, TGA oxygen losses were higher than the pulsing experiment oxygen losses for all temperatures.

Differences between oxygen losses calculated from TGA and from pulsing experiments are thought to be mainly the result of a difference in pO_2 between the 5% H_2/N_2 atmosphere used in TGA and the 20% CH_4/N_2 in the pulsing setup. Further differences are expected to have occurred because of the initial presence of carbonates and hydrates on the powders. Although powders were treated before TGA measurements, several hours passed between the removal of carbonates and the start of the TGA measurement. During this time, the samples were exposed to room-temperature air and some carbonates may have reformed on the powder surface. In case of the pulsing experiments, samples were oxidized immediately before the experiment, without exposure to room temperature air. This explains the higher oxygen loss values measured with the TGA at the lower measurement temperatures, especially for LSCMFe.

CO_2 production rates on LSCMFe continuously decreased with decreasing oxygen content, as observed for LSCM. However, CO_2, CO, and average C production rates, measured on multiple LSCMFe samples, were all consistently lower than for LSCM. One possible explanation for the lower rates is the higher firing temperature of LSCMFe powder. However, this mainly influences the area available for reaction, which is already accounted for in LSCMFe's lower BET surface area used to normalize the measured rates. Although it is difficult to accurately measure the BET area for low-surface area materials, the BET area for LSCM, which is only slightly higher than for LSCMFe, agreed very well with the value measured by Danilovic for the same material, 4.4 versus 4.3 m^2/g, respectively.[14] Measurement of the BET surface area on a sample containing twice the amount of LSCMFe did not significantly change the value for the surface area.

Another explanation is that the presence of Fe stabilized the oxygen in the LSCM lattice: not only does LSCMFe have a lower CH_4 reaction rate, also the amount of oxygen that is released from the sample is much smaller

(22) Shannon, R. D. *Acta Crystallogr., Sect. A* **1976**, *32*(SEP1), 751–767.
(23) Bastidas, D. M.; Tao, S. W.; Irvine, J. T. S. *J. Mater. Chem.* **2006**, *16*(17), 1603–1605.
(24) Sfeir, J. *J. Power Sources* **2003**, *118*(1−2), 276–285.

than for the other samples −0.17 mol O/mol LSCMFe compared to 0.34 mol O/mol LSCM at 800 °C. This was confirmed by the TGA data (table 2): at 800 °C, LSCMFe released 0.18 mol O/mol perovskite whereas LSCM (and also LSCMCo and LSCMNi) released ~0.24 mol O/mol perovskite. The higher stability of lanthanum ferrate perovskites compared to lanthanum manganate was previously reported by Gauckler.[25]

The secondary CO_2 peak observed for LSCMCo and LSCMNi did not occur on LSCM or LSCMFe and thus must be related to the presence of Co and Ni. Since the first CO_2 peak, present in all the samples, is attributed to the reduction of Mn,[10] the second peak is likely due to the reduction of Co and Ni. The observation that the second CO_2 peak occurs at 650 °C for as prepared LSCMNi, but at temperatures as low as 550 °C for previously reduced (and subsequently reoxidized) LSCMNi indicates that a nonreversible change is occurring in the sample upon treatment in reducing atmospheres. This change is also seen in the Arrhenius figure for the initial CO_2 production rates on LSCMCo and LSCMNi. The decrease in the slope of the LSCMCo and LSCMNi trendlines occurred at temperatures that are consistent with the appearance of the secondary CO_2 production peaks and indicates a decrease in activation energy with temperature.

The question is what is changing in these compounds? The appearance of the second CO_2 production peak in the case of LSCMNi and LSCMCo matched the trends observed for the LSCM+Ni sample and the initial CO_2 production rates on LSCMNi were found to increase with the temperature at which the sample was previously reduced. Both observations are very strong evidence for the exsolution of Ni and Co from the LSCMNi and LSCMCo perovskites, respectively. Although separate Co and Ni phases could not be detected by XRD or XPS, small amounts of Ni (1 wt %, comparable to 8.5 mol %) have been shown to dramatically improve SOFC power density.[11]

Surface nanoparticles were recently observed on reduced $La_{0.75}Sr_{0.25}Cr_{0.50}Mn_{0.30}Ni_{0.20}O_{3-\delta}$ by TEM.[26] However, we observed the existence of small particles on both LSCMNi and Ni-free LSCM, indicating that in our case these particles should at least in part be attributed to a non-nickel phase. EDX analysis on the small particles was attempted but did not yield conclusive results because of the small size of the particles compared to the large measurement area of the EDX. Since an RP phase was detected with XRD at temperatures slightly higher than the treatment temperatures of the TEM samples, it is likely that the small particles are an $A_2BO_{4-\delta}$ intergrowth. The as-prepared material could contain small amounts of this phase, too small to be detectable in XRD, and after treatment in reducing atmospheres, the number of these particles increased until the RP phase was detectable with XRD.

It can be concluded that the local environments of Co and Ni change at temperatures of approximately 650 and 750 °C, respectively, and that the catalytic activities of LSCMCo and LSCMNi change accordingly. Where previously Co and Ni were part of the perovskite lattice, our data suggests that at 650 and 750 °C they are either incorporated into an RP phase, or more likely, form a separate oxide phase on the surface. The observed second CO_2 production peak for LSCMNi is likely because of the reduction of surface-segregated NiO to metallic Ni, releasing oxygen anions that react with CH_4 to form CO and CO_2. SOFC tests comparing GDC/LSCM anodes with and without the addition of a separate Ni phase show a 2−5-fold increase in power output for cells with Ni added to the anode.[11,12] Such a high difference in power output does not compare to the slight increase (20%) in initial CO_2 reaction rates measured in this article for LSCMNi or LSCM+Ni compared to LSCM, but in a working fuel cell, the actual oxygen content of the material will be lower than the initial oxygen content.[8] The large difference in power output compares very well with the large difference in CO_2 and CO production rates measured for LSCMNi at lower oxygen contents, where LSCMNi produces CO_2 in a second peak, while LSCM does not produce significant amounts of CO_2.

Conclusion

LSCMX compounds (X = Co, Fe, Mn, and Ni) are stable up to 800 °C in dry 20% CH_4/N_2, at which point small amounts of a Ruddlesden−Poepper phase, $A_2BO_{4-\delta}$ phase were detected with XRD. Catalytic experiments provided indirect evidence for the exsolution of Ni and Co from their perovskite lattices at lower temperatures, > 650 and > 700 °C respectively.

The substitution of Mn with Co or Ni in the LSCM lattice increased CH_4 reaction rates, but only after the exsolution of Co and Ni from the perovskite lattice. At reduced oxygen stoichiometries, both the CO_2 and CO rates were increased by at least an order of magnitude compared to LSCM. The enhanced reaction rates of CH_4, combined with only a slight increase in cracking rates, make LSCMCo and LSCMNi good candidates for use in SOFC anodes.

Acknowledgment. This work was supported by the National Science Foundation under the Faculty Early Career Development Program (CAREER) grant CBET-0643931. The authors are grateful to M. Ali Haider for carrying out TEM measurements, Jerry Hunter at Virginia Polytechnic Institute and State University for XPS analysis, and Derek J. Bonham for sample preparation.

(25) Nakamura, T.; Petzow, G.; Gauckler, L. J. *Mater. Res. Bull.* **1979**, *14*(5), 649.
(26) Jardiel, T.; Caldes, M. T.; Moser, F.; Hamon, J.; Gauthier, G.; Joubert, O. *Solid State Ionics* **2010**, *181*(19−20), 894.